iScience

CellPress
OPEN ACCESS

Article

Single-Cell Transcriptome Analysis Dissects the Replicating Process of Pancreatic Beta Cells in Partial Pancreatectomy Model

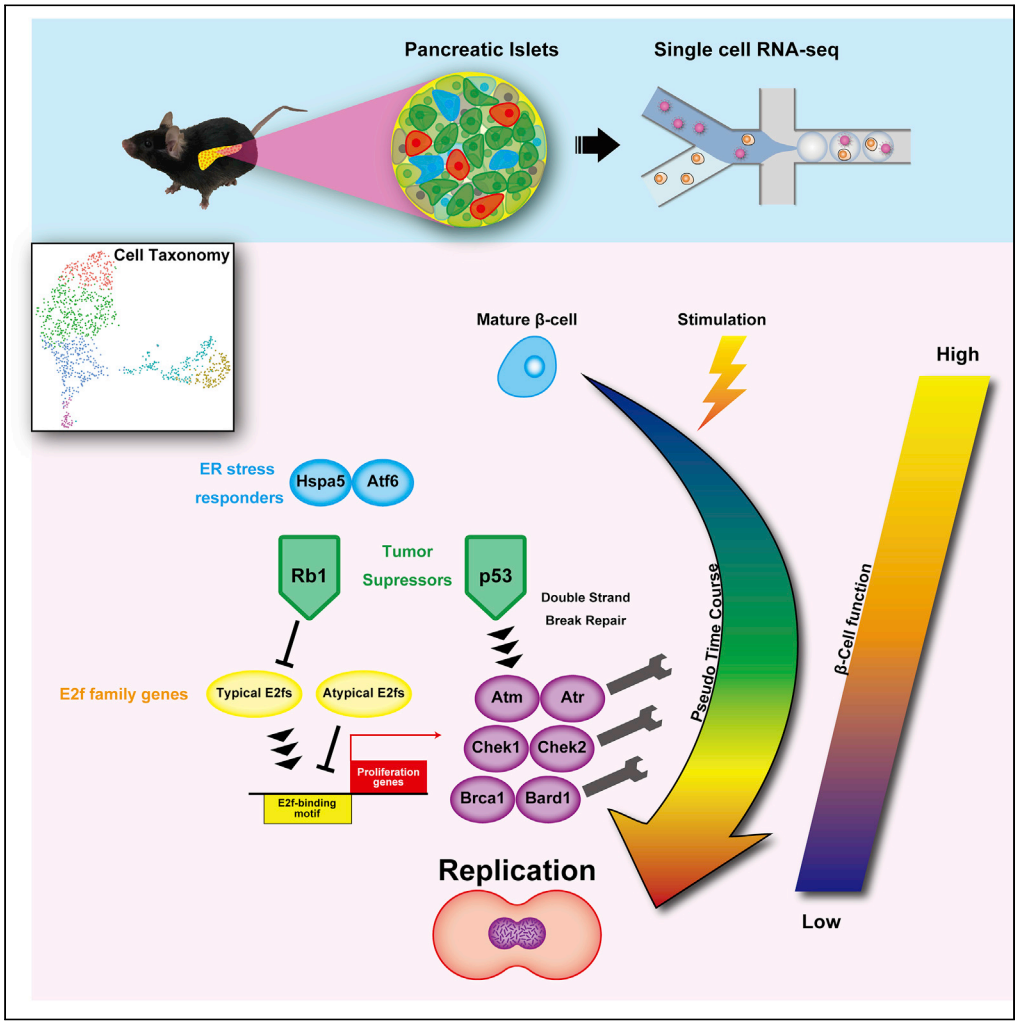

Hisato Tatsuoka, Satoko Sakamoto, Daisuke Yabe, ..., Yoshio Fujitani, Akira Watanabe, Nobuya Inagaki

inagaki@kuhp.kyoto-u.ac.jp (A.W.)
a.watanabe@aw-lab.kyoto (N.I.)

HIGHLIGHTS

Single cell RNA sequencing dissects a sequence of replication process of beta cells

ER stress responders are transiently activated in initiation of the proliferation

Physiological replication accompanied with induced expression of tumor suppressors

Fine balance of proliferation genes and tumor suppressors is a key of the replication

Tatsuoka et al., iScience *23*, 101774
December 18, 2020
https://doi.org/10.1016/j.isci.2020.101774

iScience

CellPress
OPEN ACCESS

Article

Single-Cell Transcriptome Analysis Dissects the Replicating Process of Pancreatic Beta Cells in Partial Pancreatectomy Model

Hisato Tatsuoka,[1,8] Satoko Sakamoto,[2,8] Daisuke Yabe,[1,3,4,5] Ryotaro Kabai,[2] Unyanee Kato,[2] Tatsuya Okumura,[2] Ainur Botagarova,[1] Shinsuke Tokumoto,[1] Ryota Usui,[1] Masahito Ogura,[1] Kazuaki Nagashima,[1] Eri Mukai,[6] Yoshio Fujitani,[7] Akira Watanabe,[2,*] and Nobuya Inagaki[1,9,*]

SUMMARY

Heterogeneity of gene expression and rarity of replication hamper molecular analysis of β-cell mass restoration in adult pancreas. Here, we show transcriptional dynamics in β-cell replication process by single-cell RNA sequencing of murine pancreas with or without partial pancreatectomy. We observed heterogeneity of *Ins1*-expressing β-cells and identified the one cluster as replicating β-cells with high expression of cell proliferation markers *Pcna* and *Mki67*. We also recapitulated cell cycle transition accompanied with switching expression of *cyclins* and E2F transcription factors. Both transient activation of endoplasmic reticulum stress responders like *Atf6* and *Hspa5* and elevated expression of tumor suppressors like *Trp53, Rb1, and Brca1* and DNA damage responders like *Atm, Atr, Rad51, Chek1*, and *Chek2* during the transition to replication associated fine balance of cell cycle progression and protection from DNA damage. Taken together, these results provide a high-resolution map depicting a sophisticated genetic circuit for replication of the β-cells.

INTRODUCTION

Type 2 diabetes is characterized by impaired insulin secretion resulting from dysfunction of the pancreatic β-cells and/or reduction in β-cell mass in addition to insulin resistance in peripheral tissues (Fujimoto and Inagaki, 2011; Kahn, 2003; Yabe et al., 2015). Current anti-diabetes drugs targeting β-cell dysfunction enhance insulin release from β-cells (Seino et al., 2017) but exhibit limited effect to patients whose β-cell mass is already reduced. Since developing new drugs for the patient with low β-cell mass has been highly desired, several strategies for increment of intrinsic β-cell mass are proposed, such as stimulating β-cell replication, decreasing β-cell death, and producing mature β-cells from progenitors or other types of cells (Karaca et al., 2009). Previous studies showed self-replication of pre-existing β-cells plays the most important role in the maintenance of β-cell mass in adult mice (Dor et al., 2004; Teta et al., 2007). However, replication rate of β-cells in adult human and mice is extremely low (Butler et al., 2003; Reers et al., 2009; Teta et al., 2005) as a result of its gradual decrease with aging from highest replication after birth (Gregg et al., 2012; Teta et al., 2005). Thus, an attempt to increase β-cell mass by stimulating the replication is a major challenge in the treatment of diabetes, and the mechanisms involved in β-cell replication in adult are eagerly sought.

To study molecular mechanisms of β-cell replication in adult pancreas, several animal models have been developed: acquisition of insulin resistance (El Ouaamari et al., 2016; Terauchi et al., 2007), induction of hyperglycemia (Sharma et al., 2015), pregnancy model (Kim et al., 2010), β-cell ablation (Morita et al., 2016), administration of a glucokinase activator (Nakamura et al., 2009), and partial pancreatectomy (PPTx) model (Peshavaria et al., 2006; Rankin and Kushner, 2009; Togashi et al., 2014). Among these efforts, PPTx has been shown to offer the most robust replication of murine β-cells without critical effect on blood glucose. A microarray analysis shows altered expression of cell cycle genes and the *Reg* gene family by PPTx but could not address whether the alterations recapitulated replicating β-cell-specific gene networks (Rankin and Kushner, 2010), probably due to the fact that islets are composed of multiple cell types such as α-, δ-, PP, and β-cells including a small number of replicating cells (Bader et al., 2016; Dorrell et al., 2016;

[1]Department of Diabetes, Endocrinology and Nutrition, Kyoto University Graduate School of Medicine, Kyoto, Japan

[2]Medical Innovation Center, Kyoto University Graduate School of Medicine, Kyoto, Japan

[3]Department of Diabetes and Endocrinology, Gifu University Graduate School of Medicine, Gifu, Japan

[4]Yutaka Seino Distinguished Center for Diabetes Research, Kansai Electric Power Medical Research Institute, Hyogo, Japan

[5]Division of Molecular and Metabolic Medicine, Department of Physiology and Cell Biology, Kobe University Graduate School of Medicine, Hyogo, Japan

[6]Laboratory of Medical Physiology and Metabolism, Department of Biomedical Sciences, College of Life Sciences, Ritsumeikan University, Shiga, Japan

[7]Laboratory of Developmental Biology and Metabolism, Institute for Molecular & Cellular Regulation, Gunma University, Gunma, Japan

[8]These authors contributed equally

[9]Lead Contact

*Correspondence: inagaki@kuhp.kyoto-u.ac.jp (A.W.), a.watanabe@aw-lab.kyoto (N.I.)

https://doi.org/10.1016/j.isci.2020.101774

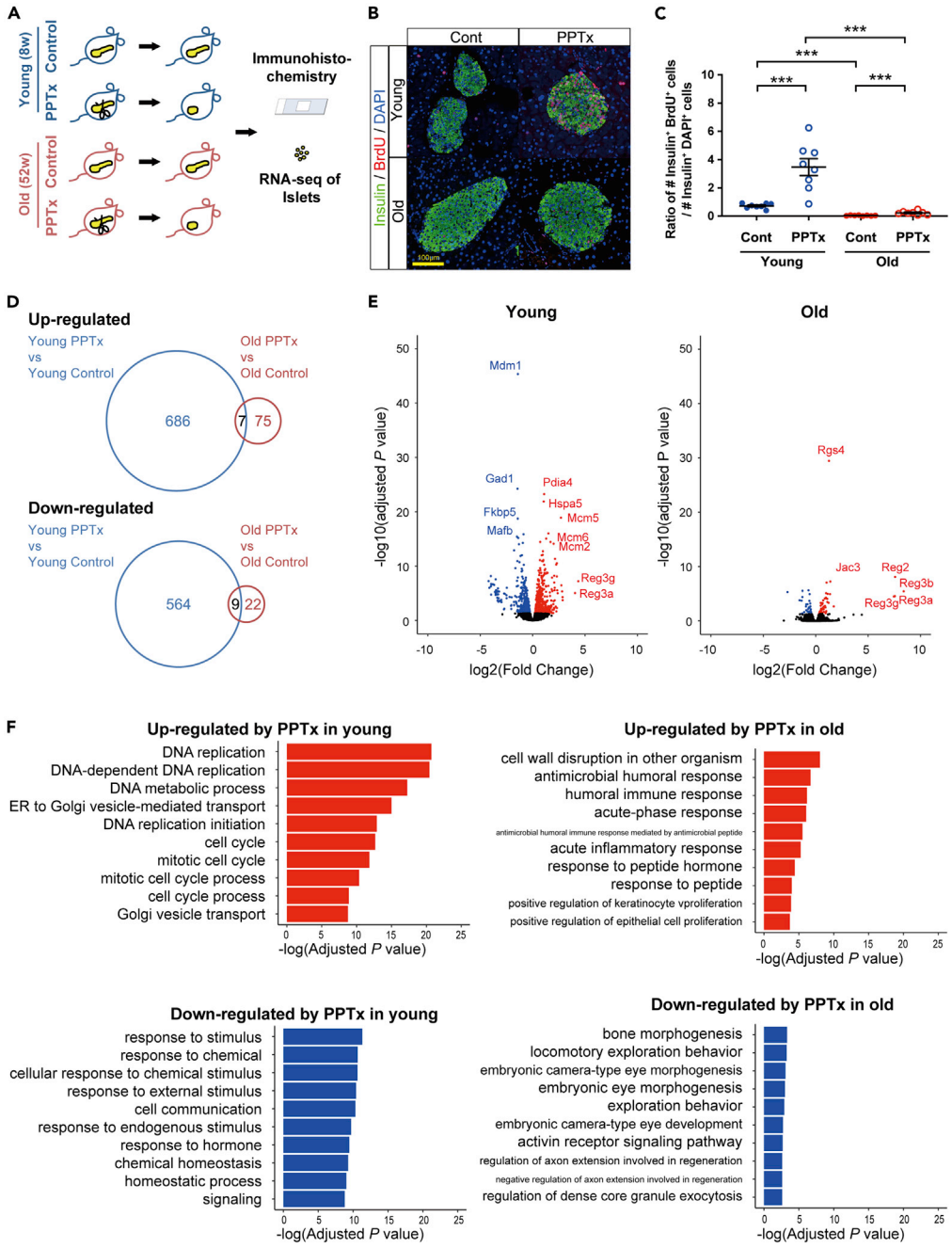

Figure 1. Altered Gene Expression Profile of Pancreatic β-cells after Partial Pancreatectomy (PPTx)

(A) Experimental design for analyses of replication of β-cells using PPTx mice. Young and old C57BL/6J mice were subjected to PPTx followed by immunohistochemistry and RNA sequencing. The control group received no surgical operation.

(B) Representative image of pancreatic β-cells labeled with 5-bromo-2′-deoxyuridine (BrdU). Scale bar represnts 100 μm. The pancreas from young and old mice in the control and PPTx groups were immunostained for insulin (green), BrdU (red), and 4′,6-diamidino-2-phenylindole (DAPI) (blue).

(C) Ratio of insulin$^+$BrdU$^+$ cells to insulin$^+$DAPI$^+$ cells. Values are mean ± SEM. ***, $p < 0.001$ (Mann-Whiteny U test).

(D) Numbers of differentially expressed genes in bulk RNA sequencing analysis between islets of control and 2 days after PPTx in young (blue) and old (red) mice (n = 4, each group). Numbers of upregulated genes (upper panel) and downregulated genes (lower panel) in the PPTx group compared to control ones were shown.

Figure 1. *Continued*

(E) Volcano plots of differentially expressed genes in bulk RNA sequencing of the control and PPTx group in young (left) and old mice (right) (n = 4, each group). Genes significantly upregulated and downregulated in PPTx groups are indicated in red and blue, respectively. Adjusted p value <0.05 was defined as significant.

(F) Gene ontology (GO) terms enriched in genes upregulated (upper panel) or downregulated (lower panel) in the PPTx group compared to control in young (left) and old (right) mice. The top 10 GO terms are shown for each comparison. See also Figure S1 and Table S1.

Johnston et al., 2016; Steiner et al., 2010). Moreover, and more importantly, understanding of similarity or difference between physiological proliferation and malignant tumorigenesis is required for secure induction of replication of functional β-cells. Molecular understanding for fine control of the proliferation, a double-edged sword, with a brake against aberrant growth leads to development of safe pharmaceuticals (Heit et al., 2006). However, physiological condition-specific proliferation signaling has not been clarified.

Single-cell RNA sequencing (scRNA-seq) has enabled to highlight β-cell subpopulations based on their gene expression profiles in human and mice (Baron et al., 2016; Muraro et al., 2016; Segerstolpe et al., 2016) and describe gradual change of transcriptome by pseudo-time course analysis (Xin et al., 2018; Zeng et al., 2017). However, dynamics of gene expression in the transition to the proliferating state remains unknown. In the current study, we employed scRNA-seq to delineate taxonomy of islet cells of young mice and addressed molecular circuit activating replication of the β-cells.

RESULTS

Alteration of Gene Expression in PPTx-Induced β-Cell Proliferation

To activate replication of β-cells, we conducted 50% PPTx on 8-week-old (young) and 52-week-old (old) C57BL/6J mice as described previously (Peshavaria et al., 2006) (Figure 1A) and observed that PPTx induced mild hyperglycemia both in young and old mice, whereas obvious changes were not seen in body weight, glucose tolerance, and insulin secretion (Figures S1A–S1D), in agreement with previous reports (Rankin and Kushner, 2009; Togashi et al., 2014). *In vivo* labeling of islet cells with 5-bromo-2′-deoxyuridine (BrdU) demonstrated that proliferating insulin$^+$/BrdU$^+$ cells were significantly increased by PPTx, and increment of the cells in young mice which underwent PPTx was much greater than that in old mice (Figures 1B and 1C), which is also in agreement with a previous study (Rankin and Kushner, 2009).

We then conducted bulk RNA-seq of PPTx and control islets in young and old mice (Figures 1D and S1E) and observed induction of *Reg3a* and *Reg3g* by PPTx both in young and old mice as reported previously (Figure 1E) (Rankin and Kushner, 2010). In addition, we found young PPTx-specific induction of a large number of genes including a well-known endoplasmic reticulum (ER) marker *Hspa5* (GRP78) and DNA replication licensing factors *Mcm2*, *Mcm5*, and *Mcm6* (Figure 1E). Gene ontology (GO) enrichment analysis also showed that genes related to cell cycle and ER function were remarkably upregulated in young mice which underwent PPTx compared to its control, whereas high expression of inflammation and immune response genes was observed in old mice which underwent PPTx (Figure 1F; Table S1).

Cell Taxonomy by Single-Cell Transcriptome Profiling Highlights Replicating β-Cells

Our conventional bulk RNA-seq could not state whether altered gene expression profiles represented the majority of islet cells or reflected strong induction of the genes in a rare population such as replicating β-cells. Thus, we conducted scRNA-seq of PPTx and control islet cells from young mice to highlight gene expression signatures of replicating β-cells. Dimensionally, reduction by uniform manifold approximation and projection (UMAP) classified the islet cells into 6 subpopulations (Figure 2A), and we defined each cluster as β-cells (*Ins1*-expressing clusters 1–4), PP- and δ-cells (*Ppy*- or *Sst*-expressing cluster 5), and α-cells (*Gcg*-expressing cluster 6) (Figures 2B and S2A). In the clusters with *Ins1* expression, a proportion of cells in the cluster 4 exhibited statistically significant difference between PPTx and control groups (Figure 2C), proposing this cluster was a replicating β-cell population. A proportion of cluster 4 cells was concordance with immunohistochemistry of BrdU$^+$ cells (BrdU$^+$, 0.73% in control vs 3.47% in PPTx; and cluster 4 cells, 2.3% in control vs 5.6% in PPTx) and exhibited high reproducibility in replicates (N = 4 in Figures 1C and 2C). Cell cycle scoring analysis also demonstrated that all cluster 4 cells were in S and G2/M phase, whereas the other β-cell clusters exhibited mixed status of cell cycle (Figures 2D and S2B; Table S2). We further confirmed high expression of cell-cycle-related genes including *Mki67* (Ki67) and *Pcna* (Figures 2E and S2C; Table S3) and concluded that cluster 4 cells were replicating β-cells. While GO analyses

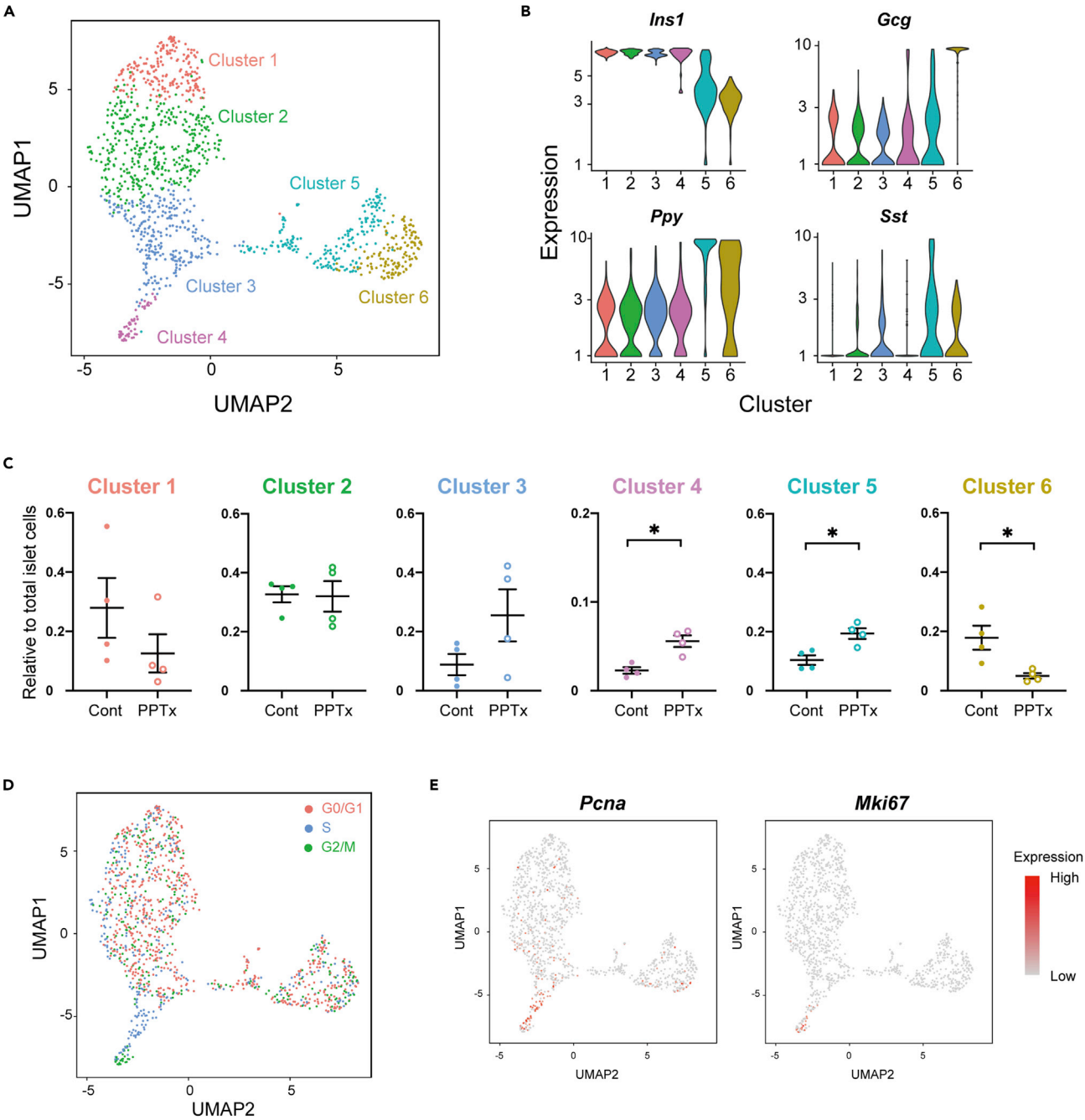

Figure 2. Cell Taxonomy and Pseudo-Time Course Analysis by Single-Cell Transcriptome Profiling of Islet Cells

(A) Uniform manifold approximation and projection (UMAP) plot of pancreatic islet cells from PPTx and control mice (PPTx, 712 cells from 4 samples; control, 520 cells from 4 samples).

(B) Gene expressions of endocrine hormones (*Ins1*, *Gcg*, *Ppy*, and *Sst*) in each cluster.

(C) Relative proportions of cell numbers in each cluster to total cell numbers. Values are mean ± SEM. *, $p < 0.05$ vs control (Mann-Whitney U test).

(D) Estimation of cell cycle in each cluster. Red color, G0/G1 phase; blue, S phase; green, G2/M.

(E) The expressions of *Pcna* and *Mki67* on UMAP plot.

also showed differential expression of cell-cycle-related genes in cluster 4 cells, dominant signatures of differentially expressed genes were downregulation of protein transport pathways in cluster 1 and upregulation of ER stress responders, such as *Hsp90b1*, *Hspa5*, *Ssr3*, and *Manf*, in cluster 3 (Figure S2C; Table S3).

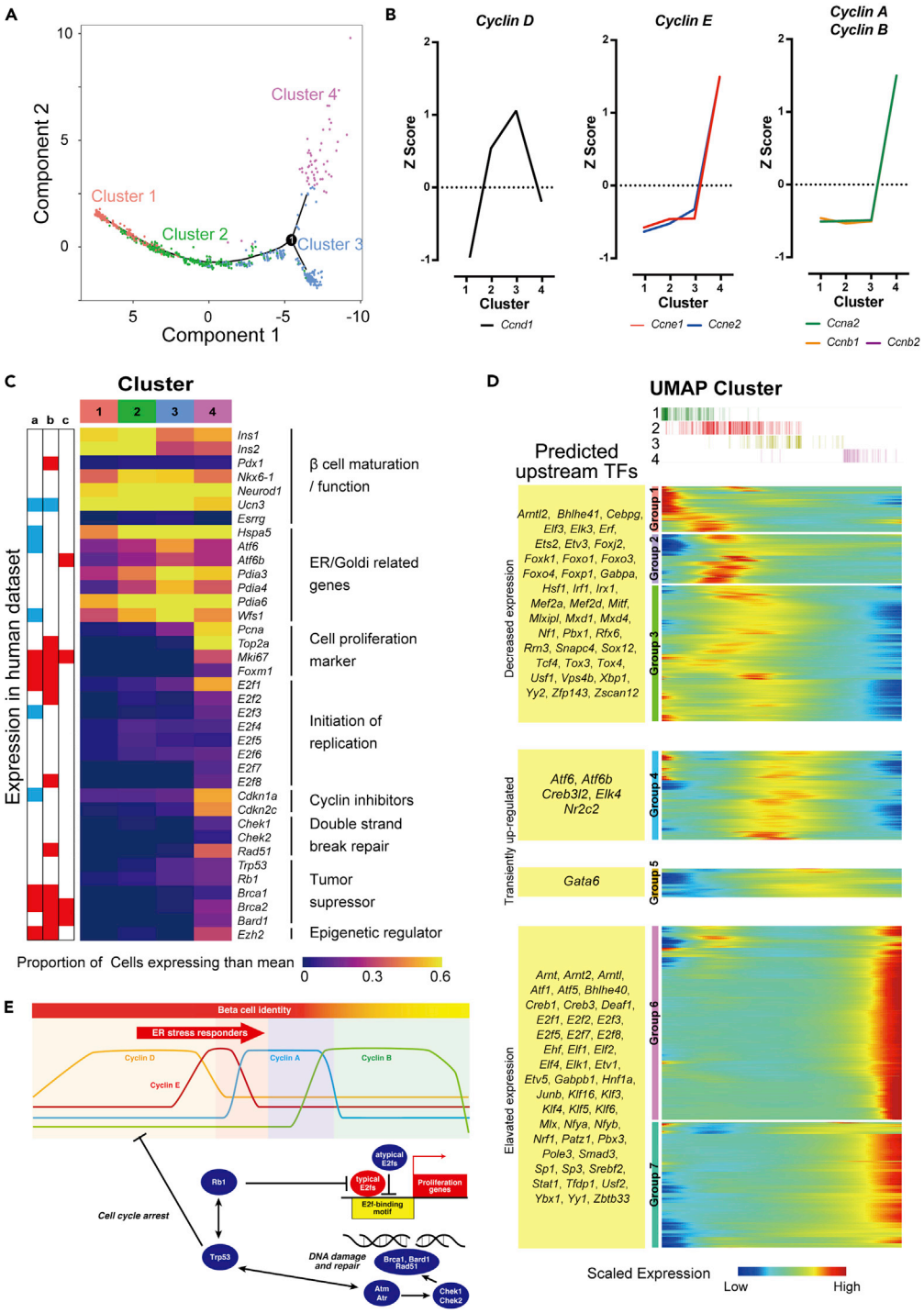

Figure 3. Dynamics of Gene Expression and Regulation in a Transition to Replication of β-cells

(A) Trajectory plot showing transition of cells from the cluster 1 through the cluster 2 and 3 to the cluster 4.

(B) Dynamic expression of cell-cycle-specific cyclins in the UMAP clusters. The *Z* score of mean expression in each cluster was shown.

(C) The expression score of genes related to β-cell maturation and function, ER stress, cell proliferation, initiation of replication, cyclin inhibitors, double-strand break repair, tumor suppressor, and epigenetic regulator in Ins1^{+} cluster on UMAP (i.e., cluster 1–4). Scores were calculated with the number of cells which expression values of the gene were more than its mean expression among cluster 1–4 cells divided by total cell numbers of individual clusters. Row annotation

Figure 3. *Continued*
located on the left shows the association to genes reported in previous studies as for human β-cell: (A) human insulinoma (Wang H, et al., 2017), (B) replication-stimulated human islets by Dyrk1a inhibitor (Ackeifi et al., 2020), and (C) juvenile human islets (Arda et al., 2016). Red, upregulated genes; blue, downregulated in proliferative tissues or cells.
(D) Dynamics of gene regulations were depicted using the pseudo-temporal expression pattern, showing a rough fit to a trajectory of the UMAP clusters. The pattern of gene expression in pseudo-time was classified into 7 groups (group 1–7). Candidate upstream regulators whose expression exhibited the same pattern of gene expression were listed on the left.
(E) Schematic of a sequence of replication process of β-cell replication with switching gene regulation. Switching expression of *cyclins* and transient activation of ER stress responders is followed by induction of a series of tumor suppressors and DNA damage responders002C as well as high expression of cell proliferation-related genes.
See also Figure S3 and Tables S6 and S7.

Activation of ER Stress and DNA Damage Responders during Transition to Proliferative State of β-Cells

Pseudo-time course analysis displayed a trajectory of the cells from cluster 1 through clusters 2 and 3 to cluster 4 (Figure 3A), demonstrating that the trajectory recapitulated a process of transition to the replicating state of the β-cells. We indeed observed switching expression of *cyclins* in a trajectory recapitulated cell cycle transition from G0/G1, S to G2/M phase (Figure 3B; Table 1): upregulation of late G1 genes *Ccnd1* from cluster 1 to cluster 2; upregulation of *Ccne2* (G1-to-S) from cluster 2 to cluster 3; bursting expression of *Ccne1*, *Ccne2*, and *Cdk2* (G1-to-S), *Ccna2* (S), and *Ccnb1*, *Ccnb2*, and *Cdk1* (G2) from cluster 3 to cluster 4. We next addressed gene networks responsible for replication of the β-cells. Detailed look of the differentially expressed genes using the ingenuity pathway analysis and GO suggested a sequential alteration of gene expression in a transition to replication of the β-cells (Figures 3C and S3A; Tables 1 and S4). ER/Golgi-related genes including *Atf6*, *Hspa5*, *Wfs1*, and *Pdia* family and a set of tumor suppressor genes *Trp53* (murine p53), *Rb1*, and *Brca1* were activated at clusters 2 and 3 (Figure 3C; Table 1). Then, expressions of E2F family genes such as *E2f1*, *E2f2*, and *E2f3*, cell proliferation markers including *Top2a*, *Pcna*, *Foxm1*, and *Mki67*, cyclin inhibitors *Cdkn1a* (p21), *Cdkn2a* ($p14^{ARF}$/$p16^{INK4A}$), and *Cdkn2c* (p18), and regulators of a double-strand break repair such as *Chek1*, *Chek2*, and *Rad51* were elevated to cluster 4 (Table 1). We also observed upregulation of epigenetic regulators like *Dnmt3a*, *Mecp2*, *Ezh2*, and *Hells* in cluster 4 (Table 1).

To address whether the transcriptional signature of β-cell replication observed in mice is modeled on replication process of human pancreatic β-cells, we compared to human insulinoma (Wang et al., 2017), Dyrk1a inhibitor-induced β-cell replication (Ackeifi et al., 2020), and juvenile human islets (Arda et al., 2016). Of 440 genes enriched in cluster 4, 68, 108, and 19 genes were overlapped, respectively, and among them, the overlapped genes included replication-related genes such as *Mki67*, *Foxm1*, *Ccna2*, *Ccnb1*, *Ccnb2*, and *Ccne2* and tumor suppressor genes *Brca1*, *Brca2*, or *Bard1* (Table S5). In addition, E2f family genes of *E2f1*, *E2f2*, or *E2f8* and epigenetic regulator *Ezh2* or *Hells* were also upregulated in human data sets (Figure 3C; Table 1).

Dedifferentiation is a process of loss of specialized function, but occasionally, dedifferentiation accompanied with acquisition of different features: one is transdifferentiation to give functional somatic cells and another is reversion of differentiation process, which gives progenitor cells that can redifferentiate into several cell types. Expressions of genes responsible for β-cell function such as *Ins1*, *Ins2*, *Pdx1*, *Nkx6.1*, *Neurod1*, *Ucn3*, and *Esrrg* were declined toward cluster 4 (Figures 3C, S2C, and S3A; Table S3), indicating dedifferentiation occurs in replicating cells, in terms of loss of function (Puri et al., 2018). We then examined a possibility of transdifferentiation or reversion to progenitors. The replicating cells did not exhibit expressions of markers of immature and/or progenitor cells such as *Neurog3* or *Oct4* and *Nanog* (Talchai et al., 2012). And expression levels of the other endocrine cells like *Gcg*, *Ppy*, or *Sst* were not altered. These observations explain that our replicating cells simply lose a function as β-cells but do not exhibit any evidence of transdifferentiation and a reversion of differentiation. Taken together, replication of the β-cell is a combined process of suppression of cell identity, activation of ER stress responders, and simultaneous upregulation of tumor suppressor genes toward cell cycle progression under surveillance of DNA damage.

We finally examined molecular mechanism of transcriptional regulation raising dynamic changes in gene expression during the transition. We examined motifs enriched on promoters of differentially expressed genes and observed high enrichment of E2F-binding motifs on promoters of cluster 4 genes (Figure S3B). While DNA-binding motif among E2F family proteins is very similar and indistinguishable, gene expression

	Cluster 1vs 2	Cluster 2 vs 3	Cluster 3 vs 4
Cell Cycle			
Ccnd1[a]	1.44	NA	NA
Ccne1	NA	NA	17.00
Ccne2	NA	2.45	6.37
Ccna2[a]	NA	NA	125.47
Ccnb1[a]	NA	NA	69.81
Ccnb2[b]	NA	NA	111.28
Cdk1[b]	NA	NA	107.92
Cdk2	NA	NA	11.08
Cdk4	0.99	NA	1.82
E2f1[a,b]	NA	1.26	5.48
E2f2[b]	7.38	0.17	20.81
E2f3	NA	NA	9.46
E2f4	1.81	NA	NA
E2f7	NA	NA	27.45
E2f8[b]	NA	NA	
Mki67[a,b,c]	NA	NA	98.93
Top2a[b]	NA	NA	171.52
Pcna	NA	4.54	6.36
Foxm1[a,b]	NA	NA	96.66
ER Stress			
Atf6	NA	1.57	0.62
Atf6b[c]	1.03	1.26	NA
Hspa5	1.45	1.57	0.73
Pdia3	1.05	1.76	NA
Pdia4	2.03	1.88	0.57
Pdia6	1.41	1.42	0.86
Wfs1	1.13	1.27	0.63
Hells[d,a,b]	NA	3.76	7.86
Tumor Suppressor/DNA Damage			
Trp53	NA	3.77	NA
Cdkn1a	NA	NA	5.64
Cdkn2a	NA	NA	
Cdkn2c	NA	2.27	15.67
Rb1	NA	1.47	NA
Brca1[a,b]	NA	∞	4.35

Table 1. List of Representative Genes Differentially Expressed between the Two Clusters

(Continued on next page)

	Cluster 1vs 2	Cluster 2 vs 3	Cluster 3 vs 4
Brca2[a,b,c]	NA	∞	20.19
Bard1[b,c]	NA	NA	76.70
Atr	NA	2.38	NA
Atm	1.77	NA	2.44
Rad51[b]	NA	NA	23.30
Chek1	NA	NA	9.63
Chek2	NA	NA	
Epigenetic Regulators			
Dnmt3a	NA	1.42	0.49
Mecp2	NA	1.32	NA
Ezh2[a,b]	∞	NA	95.95

Table 1. Continued

Fold change is calculated by dividing the cpm value of the latter cluster by that of the former cluster. NA, no statistical significance between clusters; ∞, undefined high expression because expression of the denominator gene was zero.

[a]Also included in upregulated genes in the insulinoma data set (Wang et al., 2017).

[b]Also included in upregulated genes in the human islets treated by harmine (Ackeifi et al., 2020).

[c]Also included in upregulated genes in juvenile human islets (Arda et al., 2016).

[d]Also included in Epigenetic regulators.

profile suggested that *E2f1*, *E2f2*, *E2f3*, *E2f7*, and *E2f8*, which were upregulated in cluster 4, were candidate regulators of replication-related genes through their binding motifs (Figure 3C). A further analysis of transiently expressed genes demonstrated Atf6/Atf6b-binding motifs on promoters of ER stress-related genes including *Atf6* and *Atf6b* themselves (Figure 3D; Tables 1, S6, and S7).

DISCUSSION

It has been challenging to unravel the molecular mechanisms regulating β-cell replication due to the rarity of replicating β-cells and the heterogeneity of islet cells (Teta et al., 2005). Our high-resolution map of transcriptional dynamics in transition to the replication shows switching expression of *cyclins* and identifies proliferating β-cells. We show that ER stress responders, which were reported to be involved in proliferation of murine β-cells (Sharma et al., 2015; Usui et al., 2012), expressed transiently and prior to *cyclin E*, *cyclin A*, and *cyclin B*, indicating an importance of fine protein folding and quality control during cell cycle progression. The *Wfs1*, a component of unfolded protein response complex, was transiently activated, as well as the other ER stress responders. Genomic defect of the *Wfs1* gene causes Wolfram syndrome through loss of human β-cells (Hofmann et al., 2003; Ishihara et al., 2004), supporting an importance of appropriate proteostasis in the β-cells. Notably, expression of the ER stress responders was induced by PPTx only in young mice but not in old mice (Figure S3C), concordant with low potency of murine β-cell replication with age (Aguayo-Mazzucato et al., 2017; Krishnamurthy et al., 2006; Rankin and Kushner, 2010). Dysregulation of ER stress-related genes in aged mice and diseases associates new strategies to explore drug target genes by understanding the transcriptional dynamics of β-cell replication (Naidoo et al., 2014). We show not only heterogeneous expression of ER stress-related genes in pancreatic human and murine β-cells (Baron et al., 2016; Muraro et al., 2016; Xin et al., 2018) but also sophisticated connection of ER stress signaling to the other gene networks like cell cycle regulators and DNA damage responders.

We observed complicated regulation of E2f signaling. High expression of typical E2fs, such as *E2f1*, *E2f2*, and *E2f3* (Figures 3C and Table 1), and downstream genes of the *E2fs* implied that replication of β-cells was driven by these E2f signaling (Figure S3B; Tables S4 and S7), as shown in previous reports (Fajas et al., 2004; Hanahan and Weinberg, 2000; Iglesias-Ara et al., 2015; Rady et al., 2013; Thurlings and de Bruin, 2016; Wong et al., 2011). However, we also observed that *Rb1*, a cell cycle inhibitor through binding to E2Fs, expressed prior to upregulation of *E2fs* (Table S4). Poised expression of *Rb1* for control of typical *E2fs* may contribute to adequate proliferation of the β-cells. In addition, we also observed high expression of

atypical E2F family genes *E2f7* and *E2f8* (Figure 3C), which repress expression of replication-related genes as a member of p53 signaling (Carvajal et al., 2012). Interestingly, expressions of *E2F7* and *E2F8* were also induced by Dyrk1a inhibitor that promotes replication of human β-cells (Wang et al., 2015). We have recently reported that *Rb*-deficient mice with mutant *Trp53* develop aggressive insulin-secreting tumors and die by the age of 10 months (Yamauchi et al., 2020). This indicates synergistic roles of the *Rb1* with *Trp53* in tumor suppression of the pancreatic β-cells. Bidirectional regulation of E2f signaling that is involved in both promotion and suppression of cell cycle is a paradox to be unraveled.

We observed the induction of *Trp53* expression in cluster 3, followed by high induction of p53-target genes including *Chek1* and *Chek2* in cluster 4, and also found that *Atm*, *Atr*, *Brca1*, *Brca2*, *Hells*, *Bard1*, and *Rad51*, which maintain genome integrity in response to DNA damage, were induced during the transition (Tables 1 and S4). Activation of the tumor suppressors prior to cell cycle progression may also be a gatekeeper of precise cell cycle regulation in physiological replication to avoid tumorigenicity (Figure 3E; Tables 1 and S4). We additionally observed alteration of expression of epigenetic regulators like *Dnmt3a*, *Mecp2*, *Hells*, and *Ezh2* in transition during replication process (Table 1). A previous study reported dysregulation of epigenetic factors including genomic amplification of *EZH2* and overexpression of *EZH2* promoted *CCND1*-induced proliferation of insulinoma cells in human (Wang et al., 2017), whereas declined functions of these factors with aging were previously reported in mice (Chen et al., 2009). Thus, molecular understandings of gene regulation of the epigenetic factors in β-cell replication are further challenges to complete the overall picture.

Comparing control- and PPTx-derived cells, several differences were observed, including a higher induction of ER stress-related genes in PPTx-derived cells in clusters 1, 2, 3, and 4 (Figure S3A) and a biased distribution of control- and PPTx-derived cells in cluster 4 (Table S2). Although we confirmed key findings including elevated expression of proliferation-related genes and tumor suppressors both in PPTx and control mice, PPTx might activate replication inducibly through ER stress. From another perspective, we provide transcriptional signature of physiological replication of β-cells, which was obtained from control mice without any perturbations, such as any surgical operations and genetic modification (Figure S3A). Alteration of this physiological replication in aging is the next crucial issue to be examined.

We have also considered whether the replication is driven in a subpopulation of mature β-cells with proliferation capability or follows a "stochastic" model, which says that all most of β-cells harbor potency to replicate and several cells stochastically enter in S and G2/M phases. We cannot exclude any possibility of existence of "elite" cells in clusters 1–3, although our pseudo-temporal analysis suggested transition of cells from cluster 1 to cluster 4 via clusters 2 and 3 (Figures 3A and 3D). Additional question remained is why old β-cells lose the capacity to replicate. The old mice which we employed correspond to middle-aged human, whose β-cells also lose the capacity to replicate (Dutta and Sengupta, 2016). We observed differential regulation of ER stress responders between young and old mice (Figure S3C). Since middle-age-onset diabetes is also clinically important, further study using scRNA-seq or epigenetic examination is needed (Zou et al., 2016). A map of β-cell replication process altered in aging could also be a guide for cure of diabetes.

In summary, our scRNA-seq of replication-induced islet cells addresses transcriptional dynamics of β-cell replication process at high resolution, including switching expression of cyclins, transient activation of ER stress responders, and elevated expression of proliferation-related genes. Additionally, the study provides new findings including activation of anti-proliferation signaling, such as key factors responsible for surveillance of genome integrity, orchestrated by major tumor suppressor genes. Our integrated concept for physiological induction of beta cells by both acceleration and suppression of cell proliferation will link to new strategy for regenerative medicine and drug discovery.

Limitations of the Study

In this study, we employed the PPTx model to clarify β-cell replication. The phenomena observed in this study might not apply in other models. Our research was mostly observational; the mechanism of β-cell replication requires further investigation.

Resource Availability

Lead Contact

Further information and requests for resources and reagents should be directed to and will be fulfilled by the Lead Contact, Nobuya Inagaki (inagaki@kuhp.kyoto-u.ac.jp).

MATERIALS AVAILABILITY

This study did not generate new unique reagents.

Data and Code Availability

The data sets/code generated during this study are available at NCBI Gene Expression Omnibus (GEO) accession number: GSE152730 and GSE152731.

METHODS

All methods can be found in the accompanying Transparent Methods supplemental file.

SUPPLEMENTAL INFORMATION

Supplemental Information can be found online at https://doi.org/10.1016/j.isci.2020.101774.

ACKNOWLEDGMENTS

This work was supported by grants from the Japan Society for the Promotion of Sciences (JSPS) [KAKENHI Grant Number: 17K19654 (to N.I.), 17K09825 (to D.Y.), 15K06921 and 17KT0108 (to A.W.), 18K15121(to S.S.), 16K09746 (K.N.), 26111004 (to D.Y. and K.N.), 20K21616 (to N.I., H.T., and R.U.), and 20K17531 (to H.T.)], AMED-CREST (Grant Number 20gm1210012h0001, to A.W.), Kyoto University Grant ISHIZUE (to D.Y.), Japan Diabetes Foundation Lilly Incretin Basic Research Grant (to D.Y.), and Suzuken Memorial Foundation Grant (to D.Y.). The authors thank Y. Fukuchi, M. Kitaoka, S. Kanda, S. Yasui, and M. Yoshida for their technical assistance and F. Uwamori, Y. Tanaka, and Y. Inokuchi for their secretarial assistance. The authors also thank M. Nakamura for preliminary analysis.

AUTHOR CONTRIBUTIONS

Conceptualization, H.T., S.S., D.Y., A.W., and N.I.; Software, H.T., S.S., R.K., T.O., U.K., and A.W.; Investigation, H.T., S.S., D.Y., R.K., T.O., R.U., A.B., E.M., and A.W.; Validation, S.T.; Resources, Y.F.; Data Curation, H.T. and S.S.; Writing – Original Draft, H.T., S.S., and D.Y.; Writing – Review & Editing, H.T., D.Y., A.W., and N.I.; Funding Acquisition, S.S., D.Y., M.O., K.N., A.W., and N.I.; Visualization, H.T., S.S., D.Y., R.K., U.K., and A.W.; Supervision, D.Y., A.W., and N.I.

DECLARATION OF INTERESTS

The authors declare no competing interests.

Received: August 12, 2020
Revised: October 16, 2020
Accepted: November 3, 2020
Published: December 18, 2020

REFERENCES

Ackeifi, C., Swartz, E., Kumar, K., Liu, H., Chalada, S., Karakose, E., Scott, D.K., Garcia-Ocana, A., Sanchez, R., DeVita, R.J., et al. (2020). Pharmacologic and genetic approaches define human pancreatic beta cell mitogenic targets of DYRK1A inhibitors. JCI Insight *5*, e132594.

Aguayo-Mazzucato, C., van Haaren, M., Mruk, M., Lee, T.B., Jr., Crawford, C., Hollister-Lock, J., Sullivan, B.A., Johnson, J.W., Ebrahimi, A., Dreyfuss, J.M., et al. (2017). Beta cell aging markers have heterogeneous distribution and are induced by insulin resistance. Cell Metab. *25*, 898–910.e5.

Arda, H.E., Li, L., Tsai, J., Torre, E.A., Rosli, Y., Peiris, H., Spitale, R.C., Dai, C., Gu, X., Qu, K., et al. (2016). Age-Dependent pancreatic gene regulation reveals mechanisms governing human beta cell function. Cell Metab. *23*, 909–920.

Bader, E., Migliorini, A., Gegg, M., Moruzzi, N., Gerdes, J., Roscioni, S.S., Bakhti, M., Brandl, E., Irmler, M., Beckers, J., et al. (2016). Identification of proliferative and mature beta-cells in the islets of Langerhans. Nature *535*, 430–434.

Baron, M., Veres, A., Wolock, S.L., Faust, A.L., Gaujoux, R., Vetere, A., Ryu, J.H., Wagner, B.K., Shen-Orr, S.S., Klein, A.M., et al. (2016). A single-cell transcriptomic map of the human and mouse pancreas reveals inter- and intra-cell population structure. Cell Syst. *3*, 346–360.e4.

Butler, A.E., Janson, J., Bonner-Weir, S., Ritzel, R., Rizza, R.A., and Butler, P.C. (2003). Beta-cell deficit and increased beta-cell apoptosis in humans with type 2 diabetes. Diabetes *52*, 102–110.

Carvajal, L.A., Hamard, P.J., Tonnessen, C., and Manfredi, J.J. (2012). E2F7, a novel target, is up-regulated by p53 and mediates DNA damage-dependent transcriptional repression. Genes Dev. *26*, 1533–1545.

Chen, H., Gu, X., Su, I.H., Bottino, R., Contreras, J.L., Tarakhovsky, A., and Kim, S.K. (2009). Polycomb protein Ezh2 regulates pancreatic beta-cell Ink4a/Arf expression and regeneration in diabetes mellitus. Genes Dev. *23*, 975–985.

Dor, Y., Brown, J., Martinez, O.I., and Melton, D.A. (2004). Adult pancreatic beta-cells are formed by self-duplication rather than stem-cell differentiation. Nature *429*, 41–46.

Dorrell, C., Schug, J., Canaday, P.S., Russ, H.A., Tarlow, B.D., Grompe, M.T., Horton, T., Hebrok, M., Streeter, P.R., Kaestner, K.H., et al. (2016). Human islets contain four distinct

subtypes of beta cells. Nat. Commun. *7*, 11756.

Dutta, S., and Sengupta, P. (2016). Men and mice: relating their ages. Life Sci. *152*, 244–248.

El Ouaamari, A., Dirice, E., Gedeon, N., Hu, J., Zhou, J.Y., Shirakawa, J., Hou, L., Goodman, J., Karampelias, C., Qiang, G., et al. (2016). SerpinB1 promotes pancreatic beta cell proliferation. Cell Metab. *23*, 194–205.

Fajas, L., Annicotte, J.S., Miard, S., Sarruf, D., Watanabe, M., and Auwerx, J. (2004). Impaired pancreatic growth, beta cell mass, and beta cell function in E2F1 (-/-)mice. J. Clin. Invest. *113*, 1288–1295.

Fujimoto, S., and Inagaki, N. (2011). Targeting beta-cell functions in therapy for type 2 diabetes. J. Diabetes Investig. *2*, 178–179.

Gregg, B.E., Moore, P.C., Demozay, D., Hall, B.A., Li, M., Husain, A., Wright, A.J., Atkinson, M.A., and Rhodes, C.J. (2012). Formation of a human beta-cell population within pancreatic islets is set early in life. J. Clin. Endocrinol. Metab. *97*, 3197–3206.

Hanahan, D., and Weinberg, R.A. (2000). The hallmarks of cancer. Cell *100*, 57–70.

Heit, J.J., Karnik, S.K., and Kim, S.K. (2006). Intrinsic regulators of pancreatic beta-cell proliferation. Annu. Rev. Cell Dev Biol *22*, 311–338.

Hofmann, S., Philbrook, C., Gerbitz, K.D., and Bauer, M.F. (2003). Wolfram syndrome: structural and functional analyses of mutant and wild-type wolframin, the WFS1 gene product. Hum. Mol. Genet. *12*, 2003–2012.

Iglesias-Ara, A., Zenarruzabeitia, O., Buelta, L., Merino, J., and Zubiaga, A.M. (2015). E2F1 and E2F2 prevent replicative stress and subsequent p53-dependent organ involution. Cell Death Differ. *22*, 1577–1589.

Ishihara, H., Takeda, S., Tamura, A., Takahashi, R., Yamaguchi, S., Takei, D., Yamada, T., Inoue, H., Soga, H., Katagiri, H., et al. (2004). Disruption of the WFS1 gene in mice causes progressive beta-cell loss and impaired stimulus-secretion coupling in insulin secretion. Hum. Mol. Genet. *13*, 1159–1170.

Johnston, N.R., Mitchell, R.K., Haythorne, E., Pessoa, M.P., Semplici, F., Ferrer, J., Piemonti, L., Marchetti, P., Bugliani, M., Bosco, D., et al. (2016). Beta cell hubs dictate pancreatic islet responses to glucose. Cell Metab. *24*, 389–401.

Kahn, S.E. (2003). The relative contributions of insulin resistance and beta-cell dysfunction to the pathophysiology of Type 2 diabetes. Diabetologia *46*, 3–19.

Karaca, M., Magnan, C., and Kargar, C. (2009). Functional pancreatic beta-cell mass: involvement in type 2 diabetes and therapeutic intervention. Diabetes Metab. *35*, 77–84.

Kim, H., Toyofuku, Y., Lynn, F.C., Chak, E., Uchida, T., Mizukami, H., Fujitani, Y., Kawamori, R., Miyatsuka, T., Kosaka, Y., et al. (2010). Serotonin regulates pancreatic beta cell mass during pregnancy. Nat. Med. *16*, 804–808.

Krishnamurthy, J., Ramsey, M.R., Ligon, K.L., Torrice, C., Koh, A., Bonner-Weir, S., and Sharpless, N.E. (2006). p16INK4a induces an age-dependent decline in islet regenerative potential. Nature *443*, 453–457.

Morita, A., Mukai, E., Hiratsuka, A., Takatani, T., Iwanaga, T., Lee, E.Y., and Miki, T. (2016). Distinct effects of dipeptidyl peptidase-4 inhibitor and glucagon-like peptide-1 receptor agonist on islet morphology and function. Endocrine *51*, 429–439.

Muraro, M.J., Dharmadhikari, G., Grun, D., Groen, N., Dielen, T., Jansen, E., van Gurp, L., Engelse, M.A., Carlotti, F., de Koning, E.J., et al. (2016). A single-cell transcriptome atlas of the human pancreas. Cell Syst. *3*, 385–394 e3.

Naidoo, N., Davis, J.G., Zhu, J., Yabumoto, M., Singletary, K., Brown, M., Galante, R., Agarwal, B., and Baur, J.A. (2014). Aging and sleep deprivation induce the unfolded protein response in the pancreas: implications for metabolism. Aging Cell *13*, 131–141.

Nakamura, A., Terauchi, Y., Ohyama, S., Kubota, J., Shimazaki, H., Nambu, T., Takamoto, I., Kubota, N., Eiki, J., Yoshioka, N., et al. (2009). Impact of small-molecule glucokinase activator on glucose metabolism and beta-cell mass. Endocrinology *150*, 1147–1154.

Peshavaria, M., Larmie, B.L., Lausier, J., Satish, B., Habibovic, A., Roskens, V., Larock, K., Everill, B., Leahy, J.L., and Jetton, T.L. (2006). Regulation of pancreatic beta-cell regeneration in the normoglycemic 60% partial-pancreatectomy mouse. Diabetes *55*, 3289–3298.

Puri, S., Roy, N., Russ, H.A., Leonhardt, L., French, E.K., Roy, R., Bengtsson, H., Scott, D.K., Stewart, A.F., and Hebrok, M. (2018). Replication confers beta cell immaturity. Nat. Commun. *9*, 485.

Rady, B., Chen, Y., Vaca, P., Wang, Q., Wang, Y., Salmon, P., and Oberholzer, J. (2013). Overexpression of E2F3 promotes proliferation of functional human beta cells without induction of apoptosis. Cell Cycle *12*, 2691–2702.

Rankin, M.M., and Kushner, J.A. (2009). Adaptive beta-cell proliferation is severely restricted with advanced age. Diabetes *58*, 1365–1372.

Rankin, M.M., and Kushner, J.A. (2010). Aging induces a distinct gene expression program in mouse islets. Islets *2*, 345–352.

Reers, C., Erbel, S., Esposito, I., Schmied, B., Buchler, M.W., Nawroth, P.P., and Ritzel, R.A. (2009). Impaired islet turnover in human donor pancreata with aging. Eur. J. Endocrinol. *160*, 185–191.

Segerstolpe, A., Palasantza, A., Eliasson, P., Andersson, E.M., Andreasson, A.C., Sun, X., Picelli, S., Sabirsh, A., Clausen, M., Bjursell, M.K., et al. (2016). Single-cell transcriptome profiling of human pancreatic islets in health and type 2 diabetes. Cell Metab. *24*, 593–607.

Seino, S., Sugawara, K., Yokoi, N., and Takahashi, H. (2017). beta-Cell signalling and insulin secretagogues: a path for improved diabetes therapy. Diabetes Obes. Metab. *19* (*Suppl 1*), *22–29*.

Sharma, R.B., O'Donnell, A.C., Stamateris, R.E., Ha, B., McCloskey, K.M., Reynolds, P.R., Arvan, P., and Alonso, L.C. (2015). Insulin demand regulates beta cell number via the unfolded protein response. J. Clin. Invest. *125*, 3831–3846.

Steiner, D.J., Kim, A., Miller, K., and Hara, M. (2010). Pancreatic islet plasticity: interspecies comparison of islet architecture and composition. Islets *2*, 135–145.

Talchai, C., Xuan, S., Lin, H.V., Sussel, L., and Accili, D. (2012). Pancreatic beta cell dedifferentiation as a mechanism of diabetic beta cell failure. Cell *150*, 1223–1234.

Terauchi, Y., Takamoto, I., Kubota, N., Matsui, J., Suzuki, R., Komeda, K., Hara, A., Toyoda, Y., Miwa, I., Aizawa, S., et al. (2007). Glucokinase and IRS-2 are required for compensatory beta cell hyperplasia in response to high-fat diet-induced insulin resistance. J. Clin. Invest. *117*, 246–257.

Teta, M., Long, S.Y., Wartschow, L.M., Rankin, M.M., and Kushner, J.A. (2005). Very slow turnover of beta-cells in aged adult mice. Diabetes *54*, 2557–2567.

Teta, M., Rankin, M.M., Long, S.Y., Stein, G.M., and Kushner, J.A. (2007). Growth and regeneration of adult beta cells does not involve specialized progenitors. Dev. Cell *12*, 817–826.

Thurlings, I., and de Bruin, A. (2016). E2F transcription factors control the roller coaster ride of cell cycle gene expression. Methods Mol. Biol. *1342*, 71–88.

Togashi, Y., Shirakawa, J., Orime, K., Kaji, M., Sakamoto, E., Tajima, K., Inoue, H., Nakamura, A., Tochino, Y., Goshima, Y., et al. (2014). beta-Cell proliferation after a partial pancreatectomy is independent of IRS-2 in mice. Endocrinology *155*, 1643–1652.

Usui, M., Yamaguchi, S., Tanji, Y., Tominaga, R., Ishigaki, Y., Fukumoto, M., Katagiri, H., Mori, K., Oka, Y., and Ishihara, H. (2012). Atf6alpha-null mice are glucose intolerant due to pancreatic beta-cell failure on a high-fat diet but partially resistant to diet-induced insulin resistance. Metabolism *61*, 1118–1128.

Wang, H., Bender, A., Wang, P., Karakose, E., Inabnet, W.B., Libutti, S.K., Arnold, A., Lambertini, L., Stang, M., Chen, H., et al. (2017). Insights into beta cell regeneration for diabetes via integration of molecular landscapes in human insulinomas. Nat. Commun. *8*, 767.

Wang, P., Alvarez-Perez, J.C., Felsenfeld, D.P., Liu, H., Sivendran, S., Bender, A., Kumar, A., Sanchez, R., Scott, D.K., Garcia-Ocana, A., et al. (2015). A high-throughput chemical screen reveals that harmine-mediated inhibition of DYRK1A increases human pancreatic beta cell replication. Nat. Med. *21*, 383–388.

Wong, J.V., Dong, P., Nevins, J.R., Mathey-Prevot, B., and You, L. (2011). Network calisthenics: control of E2F dynamics in cell cycle entry. Cell Cycle *10*, 3086–3094.

Xin, Y., Dominguez Gutierrez, G., Okamoto, H., Kim, J., Lee, A.H., Adler, C., Ni, M., Yancopoulos, G.D., Murphy, A.J., and

Gromada, J. (2018). Pseudotime ordering of single human beta-cells reveals states of insulin production and unfolded protein response. Diabetes *67*, 1783–1794.

Yabe, D., Seino, Y., Fukushima, M., and Seino, S. (2015). Beta cell dysfunction versus insulin resistance in the pathogenesis of type 2 diabetes in East Asians. Curr. Diab Rep. *15*, 602.

Yamauchi, Y., Kodama, Y., Shiokawa, M., Kakiuchi, N., Marui, S., Kuwada, T., Sogabe, Y., Tomono, T., Mima, A., Morita, T., et al. (2020). Rb and p53 execute distinct roles in the development of pancreatic neuroendocrine tumors. Cancer Res. *80*, 3620–3630.

Zeng, C., Mulas, F., Sui, Y., Guan, T., Miller, N., Tan, Y., Liu, F., Jin, W., Carrano, A.C., Huising, M.O., et al. (2017). Pseudotemporal ordering of single cells reveals metabolic control of postnatal beta cell proliferation. Cell Metab. *25*, 1160–1175.e11.

Zou, W., Ni, L., Lu, Q., Zou, C., Zhao, M., Xu, X., Chen, H., and Zheng, Z. (2016). Diabetes onset at 31-45 Years of age is associated with an increased risk of diabetic retinopathy in type 2 diabetes. Sci. Rep. *6*, 38113.

iScience, Volume *23*

Supplemental Information

Single-Cell Transcriptome Analysis Dissects the Replicating Process of Pancreatic Beta Cells in Partial Pancreatectomy Model

Hisato Tatsuoka, Satoko Sakamoto, Daisuke Yabe, Ryotaro Kabai, Unyanee Kato, Tatsuya Okumura, Ainur Botagarova, Shinsuke Tokumoto, Ryota Usui, Masahito Ogura, Kazuaki Nagashima, Eri Mukai, Yoshio Fujitani, Akira Watanabe, and Nobuya Inagaki

Figure S1

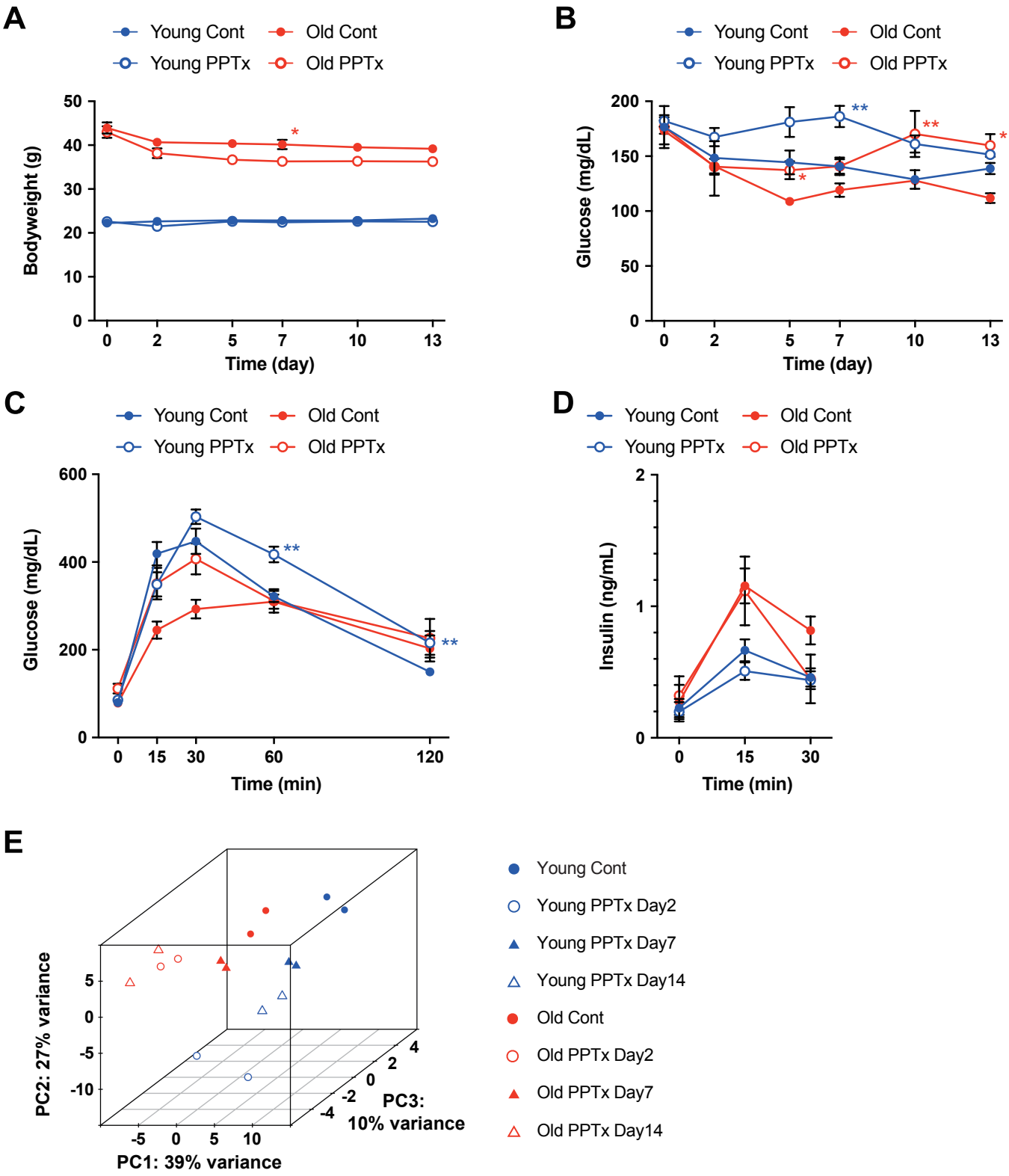

Figure S1. Phenotypical changes of young and old mice by partial pancreatectomy (PPTx).
(A) Changes of body weight. (B) Casual blood glucose levels. (C, D) Oral glucose tolerance test was performed 2 weeks after starting the observation: Levels of glucose (C) and insulin (D) were plotted. Numbers of mice examined were young control n=5, young PPTx n=5, old control n=5 and old PPTx n=4. Values are means±SEM. * and ** indicate $P < 0.05$ and $P < 0.01$ (vs control, Mann-Whitney U test), respectively. (E) PCA plot of bulk RNA-sequencing. Islets were isolated 2, 7 and 14 days after the surgical operation in PPTx mice. Related to Figure 1.

Figure S2

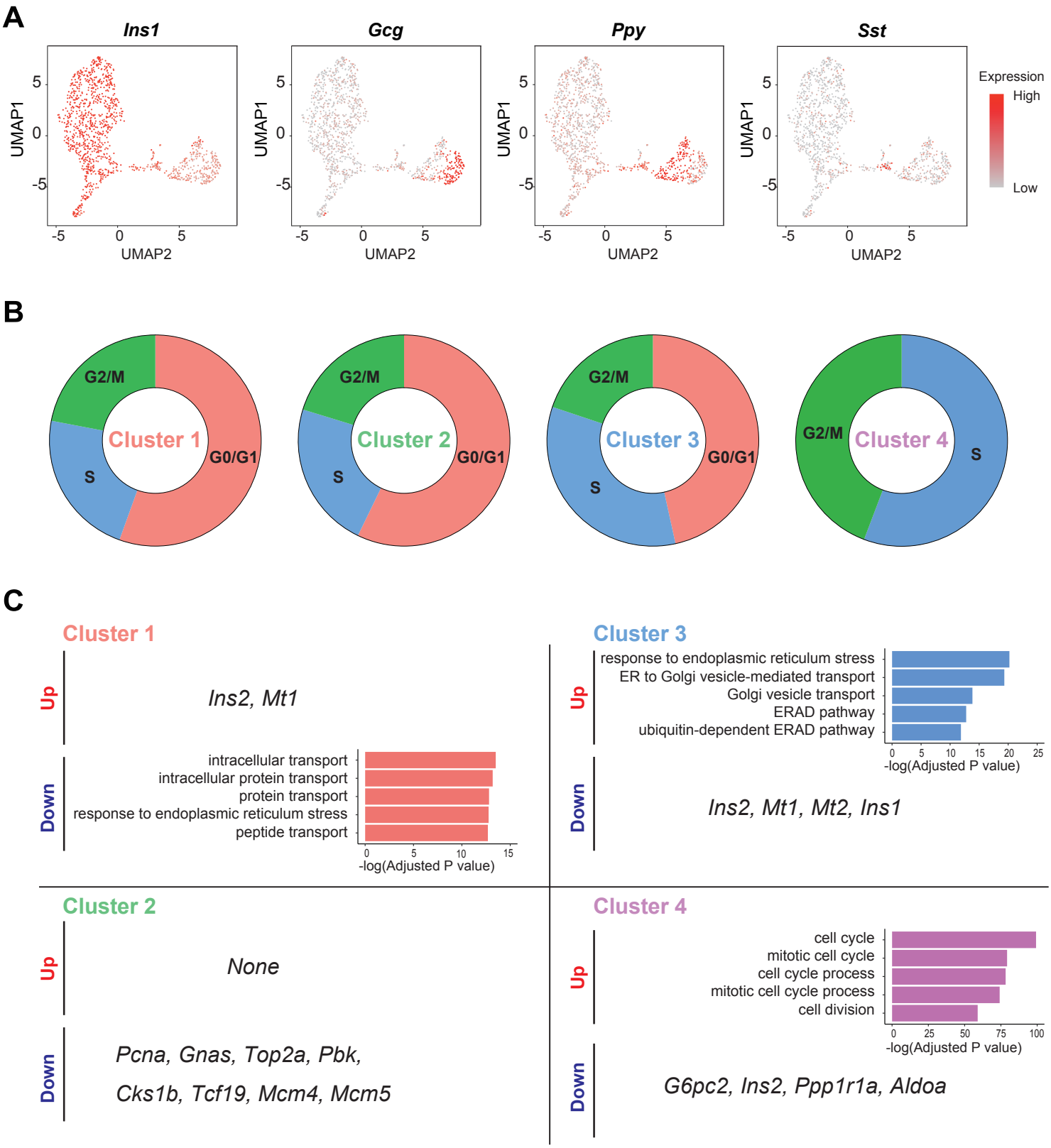

Figure S2. Cell taxonomy and cell cycle state of islet cells in young control and PPTx mice.
(A) Expressions of *Ins1*, *Gcg*, *Ppy* and *Sst* were shown on UMAP plot. (B) CellCycleScoring-defined Composition of G0/G1, S and G2/M cells in each UMAP Cluster. (C) GO terms significantly enriched in up-regulated or down-regulated genes. Gene names were listed when no significant GO term was enriched in their differentially expressed genes. All results were shown in Table S2. Related to Figure 2.

Figure S3

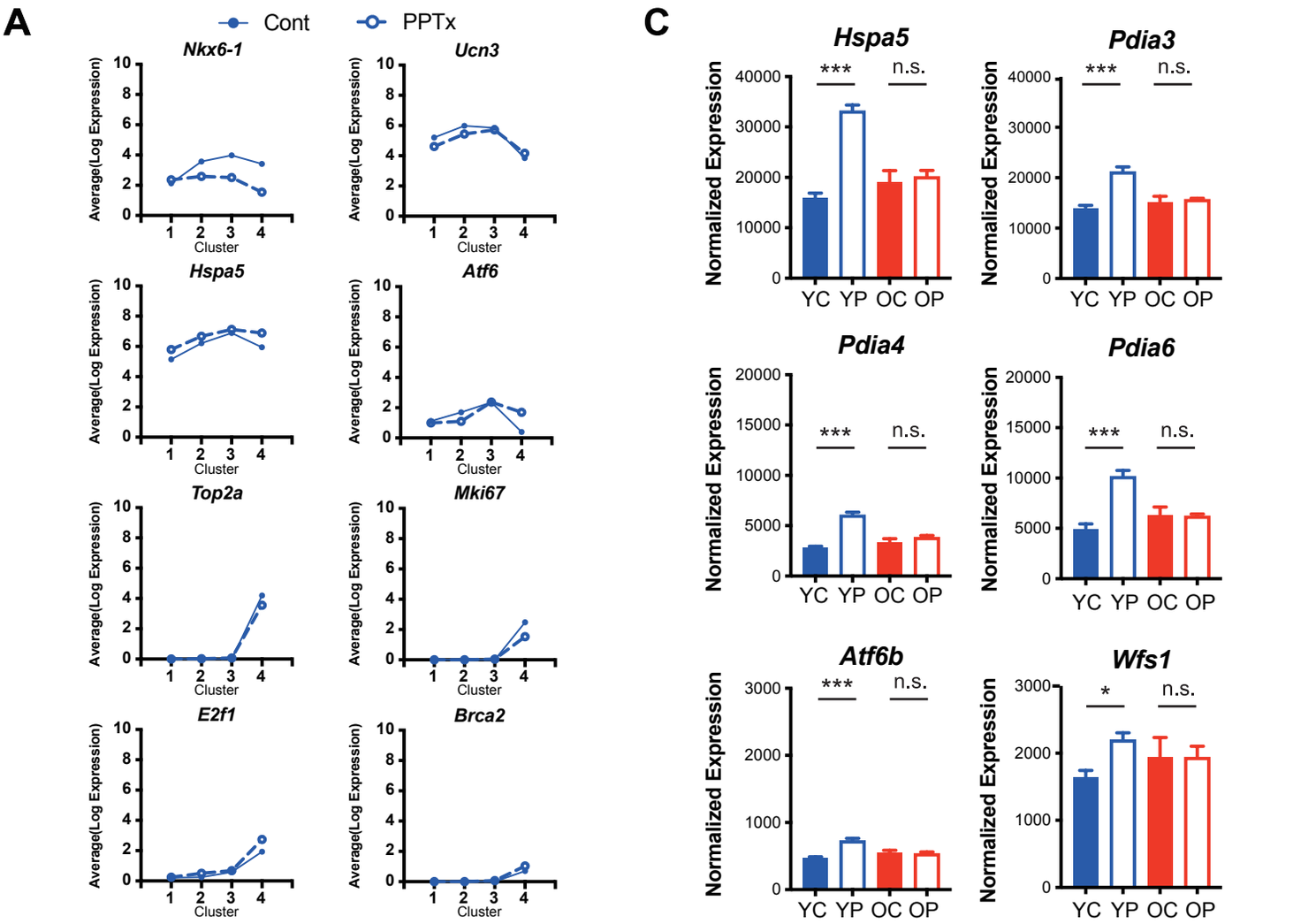

B

Cluster 1 → 2 up	TF	P value	Cluster 2 → 3 up	TF	P value	Cluster 3 → 4 up	TF	P value
	Elk1	1e-89		Elk1	1e-108		NFY	1e-50
	ELF1	1e-86		Elk4	1e-107		E2F7	1e-45
	Elk4	1e-85		ELF1	1e-100		E2F4	1e-41
	ETS	1e-84		ETS	1e-92		E2F1	1e-35
	Fli1	1e-61		Fli1	1e-74		Sp1	1e-31
	GABPA	1e-58		GABPA	1e-65		KLF1	1e-25
	Sp1	1e-57		ETV4	1e-64		E2F3	1e-24
	ETV4	1e-53		Sp1	1e-61		E2F	1e-24
	Ronin	1e-44		ETV1	1e-51		KLF3	1e-24
	GFY-Staf	1e-43		Elf4	1e-44		Sp5	1e-22

Figure S3. A sequential alteration of gene expression in a transition to replication and candidates regulating a gene network.
(A) The alteration of representative gene expressions both in control and PPTx group. Values indicates the average of the logarithm expressions. (B) Upstream motifs of differentially up-regulated genes in cluster 2 compared to cluster 1, in cluster 3 to 2 and in cluster 4 to 3 were predicted using HOMER. Top 10 results were shown. (C) Normalized expression values of ER stress related genes in bulk RNA-seq analysis were shown. YC indicates young control, YP does young PPTx, OC does old control and OP does old PPTx. Values are mean ± SEM. *, $P < 0.05$, ***, $P < 0.001$ (Mann-Whitney U test). Related to Figure 3.

Table S2. CellCycleScoring-defined Composition of G0/G1, S and G2/M cells in each UMAP Cluster of control and PPTx islets. Related to Figures 2D and S2B.

The number of cells assigned to each phase of cell cycle was divided by total number of cells in the Cluster 1-4.

	G1	S	G2M	Total cell number
Control				
Cluster 1	63.4%	17.0%	19.6%	112
Cluster 2	69.5%	11.9%	18.6%	177
Cluster 3	65.5%	17.2%	17.2%	58
Cluster 4	0%	23.1%	76.9%	13
PPTx				
Cluster 1	54.5%	30.7%	14.8%	88
Cluster 2	50.7%	30.5%	18.8%	213
Cluster 3	43.6%	36.3%	20.1%	204
Cluster 4	0%	64.1%	35.9%	39

TRANSPARENT METHODS

- KEY RESOURCES TABLE
- CONTACT FOR REAGENT AND RESOURCE SHARING
- EXPERIMENTAL MODEL AND SUBJECT DATAILS
  - Animals
- METHOD DETAILS
  - Partial Pancreatectomy
  - Histological analyses
  - Islet isolation and RNA extraction
  - Bulk RNA sequencing analysis (Bulk RNA-seq)
  - Single-cell mRNA sequencing analysis (scRNA-seq)
  - Data analysis
- QUANTIFICATION AND STATISTICAL ANALYSIS
- DATA AVAILABILITY

CONTACT FOR REAGENT AND RESOURCE SHARING

Reagents and resources included in the current study are available from the corresponding author on reasonable request. All requests will be fulfilled by Nobuya Inagaki (inagaki@kuhp.kyoto-u.ac.jp).

KEY RESOURCES TABLE

REAGENT or RESOURCE	SOURCE	IDENTIFIER
Antibodies		
Rabbit anti-insulin	Abcam	Cat#ab181547
Rat anti-BrdU	Abcam	Cat#ab6326
Chemicals, Peptides, and Recombinant Proteins		
5-Bromo-2′-deoxyuridine (BrdU)	Sigma-Aldrich	Cat# B5002-5G
Trypsin-EDTA	Thermo Fisher Scientific	Cat#15400-054
RPMI 1640 medium	Thermo Fisher Scientific	Cat#31800-022
Critical Commercial Assays		
UltraSensitive PLUS Mouse Insulin ELISA	Morinaga	Cat#49170-53
SMARTer Ultra Low Input RNA Kit for Sequencing - v3	Takara Bio Inc.	Cat#634851
Nextera XT DNA Sample Preparation kits	Illumina	Cat#FC-131-1096
SureCell WTA 3′ Library Prep Kit for the ddSEQ System	Illumina	Cat#20014279
Qubit RNA HS Assay Kit	Thermo Fisher Scientific	Cat#Q32855
Agilent RNA 6000 Pico Kit	Agilent Technologies, Inc.	Cat#5067-1513

High Sensitivity D5000 ScreenTape	Agilent Technologies, Inc.	Cat#5067-5592
Deposited Data		
Raw data files for RNA sequencing	NCBI Gene Expression	GSE152730 GSE152731
Experimental Models: Organisms/Strains		
Mouse: C57BL/6	Japan SLC, Inc.	
Software and Algorithms		
R−3.5	R project	https://www.r-project.org
Seurat-3.1	Satija lab	https://satijalab.org/seurat
Monocle-2.4	Trapnell lab	http://cole-trapnell-lab.github.io/monocle-release/
HISAT2-2.0	Pertea et al. 2016.	https://ccb.jhu.edu/software/hisat2/manual.shtml
HTSeq-0.8	Anders, Pyl, and Huber 2015.	https://htseq.readthedocs.io/en/master/
biocManager-1.30	Bioconductor project	https://bioconductor.org
DESeq2-1.22	Love, Huber, and Anders 2014.	https://bioconductor.org/packages/release/bioc/html/DESeq2.html
GOseq-1.34	Young et al. 2010.	https://bioconductor.org/packages/release/bioc/html/goseq.html
Cell Ranger-2.1	10x Genomics	

Ingenuity Pathway Aanalysis (IPA)	QIAGEN	https://digitalinsights.qiagen.com/products-overview/discovery-insights-portfolio/analysis-and-visualization/qiagen-ipa/
HOMER-4.1	Benner Lab	http://homer.ucsd.edu/homer/motif/
iReguron-1.3	Stein Aerts Lab	http://iregulon.aertslab.org
GraphPad PRISM 8	GraphPad Software	https://www.graphpad.com/scientific-software/prism/
BZ Analyzer	KEYENCE	

EXPERIMENTAL MODEL DETAILS AND SUBJECT DATAILS

Animals

C57BL/6J male mice were purchased from SLC Japan, Inc. (Hamamatsu, Japan). Animals were housed in a 14h light-10h dark cycle with free access to water and standard chow. Experiments on animals were approved by the Animal Research Committee of Kyoto University Graduate School of Medicine (MedKyo18249) and all experiments were performed in accordance with relevant guidelines and regulations of the Animal Research Committee of Kyoto University Graduate School of Medicine.

METHOD DETAILS

Partial pancreatectomy (PPTx)

PPTx was performed on 8-week-old and 52-week-old male C57BL/6J mice as described previously (Peshavaria et al., 2006). Mice were anesthetized with isoflurane inhalation, and a midline abdominal incision was made. The splenic side of the pancreas was excised partially via the line between the pylorus ring and the small intestine, after breaking mesenteric connections from the pancreas to the greater curvature of the stomach, the pylorus ring, the colon and the retroperitoneum. The weight of the resected pancreas was approximately 50% of that of total pancreas estimated by those of mice of the same age and similar bodyweight. Mice at the same age without any operation were examined as control. Body weight and casual blood glucose via tail vein using Glutest Neo Sensor (Sanwa Kagaku Kenkyusho, Japan) were examined before and until 13 days after the operation. Oral glucose tolerance test was performed at 9 a.m. on day 14 after fasting mice from 5 p.m. on the previous day. Mice were dosed orally with 2g/kg glucose, and blood samples were collected at various time points using heparinized calibrated glass capillary tubes (Catalogue No. 2-000-044-H; Drummond Scientific Company). Blood glucose levels were determined using Glutest Neo Sensor. Plasma samples were prepared by centrifugation of the blood samples at 9,000xg for 10min, and were subjected to insulin measurement using UltraSensitive PLUS Mouse Insulin ELISA kit (Catalogue No. 49170-53; Morinaga, Tokyo, Japan).

Histological analyses

The β-cell replication rate was estimated immunohistochemically by 5-bromo-2′-deoxyuridine (BrdU) labeling as previously described with minor modifications (El Ouaamari et al. 2013). Water containing 1mg/mL BrdU (Catalogue No. B5002; Merck KGaA, Darmstadt, Germany) was supplied for 4 days before the dissection or intraperitoneal injection of 100 mg/kg BrdU was done 6 hours before the dissection. The resected pancreatic tissues were fixed with 4% paraformaldehyde and embedded in paraffin. After deparaffinization, antigen-retrieval by heating in 10mM citrate buffer (pH 6.0) and blocking by blocking buffer (PBS with 10% Goat Serum and 0.2% Triton X-100), five slices (more than 120 μm apart) of each pancreas were incubated at room temperature overnight with primary antibodies [i.e., rabbit anti-insulin antibody (Catalogue No. ab181547; Abcam, USA; 200-fold dilution in blocking buffer) and rat anti-BrdU antibody (Catalogue No. ab6326; Abcam, USA; 100-fold dilution in blocking buffer)] and then for 1hr at room temperature with secondary antibodies [i.e., Alexa Fluor 488-conjugated goat anti-rabbit IgG (H+L) antibody (Catalogue No. A-11034; Thermo Fisher Scientific, USA; 200-fold dilution in blocking buffer) and Alexa Fluor 546 goat anti-rat antibody (Catalogue No. A-11081; Thermo Fisher Scientific, USA; 200-fold dilution in blocking buffer)]. The samples were washed 4 times with PBS and then incubated with PBS containing 4',6-diamidino-2-phenylindole (DAPI) at the final concentration of 0.01 mg/mL for 15 min at room temperature. The samples were then washed 4 times with PBS and mounted using VECTASHIELD Mounting Medium (Catalogue No. H-1000; VECTOR LABORATORIES, INC., USA). Each slide was observed using BZ-X700 (KEYENCE, Japan) through filters (470/40 -DM 495- 525/50: FITC), (545/25 -DM 565- 605/70: mTIRC) and (360/40 -DM 400- 460/50: DAPI). More than 10 islets per slide (>50 slides per one mouse) were analyzed; the ratio of BrdU positive cell number to cell number estimated by DAPI in pancreatic islets was calculated by BZ Analyzer (KEYENCE, Japan).

Islet isolation and RNA extraction

Islets of Langerhans were isolated by the collagenase digestion technique (Sutton et al., 1986; Usui et al., 2019). Briefly, Hanks' balanced salt solution (HBSS) (Catalogue No. 05905; Nissui Pharmaceutical Co., Ltd. Tokyo, Japan) containing 5 mM $NaHCO_3$ and 0.5 mg/ml (weight/volume)

collagenase P (Catalogue number 11213865001, Roche) was injected to the mouse pancreas via the bile duct. Subsequently, the pancreas was removed and further digested in a 50 mL tube in a shaking water bath at 37℃ for 30 min. The digested pancreas was washed 2 times by ice-cold Krebs–Ringer bicarbonate (KRB) buffer [129.4 mM NaCl, 5.2 mM KCl, 2.7 mM CaCl2, 1.3 mM KH_2PO_4, 1.3 mM $MgSO_4$, and 24.8 mM $NaHCO_3$ (pH 7.4)] equilibrated with 5% CO_2/95% O_2 and containing 2.8 mM glucose, and then suspended in 4 ml of histopaque 1119 (Catalogue number 11191, Sigma) and transferred to a clean glass tube. Two ml of histopaque 1077 (Catalogue number 10771, Sigma) and 2 ml of histopaque 1050 (prepared by mixing two volumes of histopaque 1077 with one volume of distilled water) were then sequentially overlaid to perform density gradient separation. After 800×g centrifugation for 10 min at room temperature, the islets found in the inter-phase between histopaque 1050 and histopaque 1077 were collected and washed 2 times in ice-cold KRB buffer. The resulting islets were transferred to a large dish filled with approximately 50 ml of ice-cold KRB buffer and hand-picked into a 1.5-ml tube before total RNA preparation. After 200×g centrifugation for 1 min at 4℃ and removal of supernatant, a tissue pellet was made and frozen in liquid nitrogen with RNAlater Stabilization Solution (Catalogue number 7020, Thermo Fisher Scientific).

Bulk RNA sequencing (Bulk RNA-seq)

Total RNA was prepared from the frozen pellets of isolated islets using RNeasy mini kit following the manufacture's instruction (Catalogue number 74104, Qiagen); the RNA concentration was measured using the Qubit RNA HS Assay Kit (Catalogue number Q32855, Thermo Fisher Scientific). Quality of total RNA was assessed by Agilent 2100 Bioanalyzer System (Agilent Technologies, Inc., Santa Clara, CA, USA) with Agilent RNA 6000 Pico Kit (catalogue number 5067-1513, Agilent Technologies, Inc.), and RNA samples with RNA Integrity Number (RIN) value more than 7.5 were subjected to bulk RNA-seq. Bulk RNA-seq of whole islets was performed using 10 ng of total RNA from isolated islets. Each sample of islets were collected from 1-2 mice. Total RNA was reverse transcribed with SMARTer Ultra Low Input RNA Kit for Sequencing - v3 (catalogue number 634851, Takara Bio Inc.), and libraries were prepared with Nextera XT DNA Sample Preparation kits (Catalogue number FC-131-1096, Illumina). The libraries were sequenced by Hiseq2500 following the manufacturer's instruction. Single read 93-8-8bp were mapped to the UCSC mouse transcriptome reference (mm9) by HISAT2 (version 2.0.5) (Pertea et al., 2016) and uniquely aligned reads within Ensembl gene annotations were used to quantify gene expressions as counts using HTSeq (version 0.8.0) (Anders et al., 2015). For principal component analysis, islets of control, 2, 7 and 14 days after PPTx both in young and old mice were sequenced and normalized by DESeq2 (1.22.2) (Love et al., 2014) (n=2, each group). Differentially expressed analyses were conducted between islets of control and 2 days after PPTx both in young and old mice using DESeq2 (1.22.2) and the genes of adjusted *P* values < 0.05 were defined as differentially expressed genes (DEGs) (n=4, each group). Following Gene Ontology analysis of obtained DEGs was performed using GOseq (version 1.34.1) (Young et al., 2010).

Single-cell mRNA sequencing (scRNA-seq)

More than 120 isolated islets from 1 to 3 mice per sample were collected into 0.5mL tubes in RPMI 1640 medium (Catalogue No. 31800-022; Thermo Fisher Scientific, USA) containing 10% fetal bovine serum (FBS), 10 mM HEPES, 5 mM $NaHCO_3$, 1 mM sodium pyruvate, 100 U/ml penicillin, 100 mg/ml streptomycin and 11.1 mM glucose on ice. Four samples as control and four samples as PPTx group were prepared. After 200×g-centififugation for 1 min at 4℃, the collected islets were washed once in 500 μL of calcium/magnesium free (CMF) buffer (136.9 mM NaCl, 4.0 mM KCl, 11.9 mM $NaHCO_3$, 11.1 mM glucose, and 0.42 mM NaH_2PO_4, 0.18 mM KH_2PO_4). The islets were then resuspended in 200 μL of CMF containing 2 μL of 0.5% (wt/vol) Trypsin-EDTA (Catalogue number 15400-054, Thermo Fisher Scientific) (final concentration, 0.005%), incubated for 3 min at 37℃ in a water bath, and dispersed by pipetting 50 times using a Gilson P200 pipet and 200 μl-pipet tips (Catalogue number 7231, WakenBtech Co., Ltd.). Cells were collected at the bottom of 0.5 mL tubes by 1000×g centrifugation for 5 min at 4℃ and resuspended in CMF before being applied. Cell numbers were counted by TC20 Automated Cell Counter (Bio-Rad Laboraroties, Inc.) and observed with a polarized light microscope. Single cell isolation was performed by applying dissociated islet cells to a ddSEQ Single-Cell Isolator (Bio-Rad Laboratories, Inc., USA) as described previously (Romagnoli et al., 2018). Libraries were prepared by SureCell WTA 3′

Library Prep Kit for the ddSEQ System (Catalogue number 20014279, Illumina, Inc., USA) using approximately 12,500 cells in single-cell resuspension as described previously (Tran et al., 2019). Single-cell droplets encapsulated in oil with Barcode Suspension Mix and Cell Suspension Mix were brought to reverse transcription. Second strand synthesis was conducted using the library of first strand cDNA. Quality of amplified library was assessed by Agilent 2200 TapeStation (Agilent Technologies, Inc.) with High Sensitivity D5000 ScreenTape (Catalogue number 5067-5592, Agilent Technologies, Inc.). DNA were tagged with DNA adaptors and amplified, followed by sequencing on Hiseq2500 as the manufacturer's instructions. FASTQ files were made using bcl2fastq v2.20.0.422. Paired end 68-8-0-75 bp were aligned to the mouse reference genome mm10, followed by filtering, debarcoding and UMI counting using the Cell Ranger v2.1.0 pipeline (10X Genomics).

Data analysis

scRNA-seq data analysis was conducted using R version 3.5.1 and Seurat Version 3.1(Butler et al., 2018; Stuart et al., 2019). Cells were removed if the number of detected genes was less than 100 or more than 3000, or read count was less than 100 or more than 20000. Genes were also removed if they were expressed in less than 3 cells. Normalization, scaling, dimensional reduction and clustering by PCA and UMAP were processed on Seurat pipeline as follows. After removing unwanted cells, gene expressions were normalized by for each cell by the total expression, multiplied by 10,000 and their natural logarithm were taken. Top 2000 highly variable genes calculated by FindVariableFeatures function with vst selection, were used for following PCA analysis using RunPCA function. The distance between cells were calculated using FindNeighbors function with dimension 1 to 7. Clustering was performed using FindClusters function with 0.5 as the resolution. Finally, clustered cells were plotted on UMAP space using RunUMAP function. For cell taxonomy, the expressions of *Ins1*, *Gcg*, *Ppy* and *Sst* were used as previously described (Butler et al., 2018). Cluster specific genes were calculated by FindAllMarkers function using Wilcoxon rank sum test in Seurat package and adjusted *P* value < 0.05 was defined as significant. GO analysis for cluster specific genes were conducted using goseq. Cell cycle analysis was conducted using CellCycleScoring function with a dataset in a previous report as guided on developers' website (Nestorowa et al., 2016).

Pseudo-time analysis was conducted using Monocle version 2.4.0 (Qiu et al., 2017; Trapnell et al., 2014). Cells of β-cell populations (i.e., Cluster 1-4) and filtered genes on UMAP analysis (i.e., expressed in at least 3 cells) were used. Pseudo-time of each cell was calculated by reduceDimension function by DDRTree method. Genes for ordering were selected by q value less than 0.05 by differentialGeneTest function following to reduceDimension and clusterCells without marker genes as unsupervised manner. After plotting the trajectory along with pseudo-time, cells from cluster 1 to 4 were selected and the scaled expression of all genes were drawn using plot pseudo-time heatmap function. All genes were classified into 7 groups depending on their expression patterns. GO terms enriched in genes of each cluster were calculated by GOseq. Dynamic expression of cell cycle-specific *cyclins* was shown as Z score of mean expression in each cluster.

Pathway analysis was conducted using Ingenuity Pathway Analysis (IPA, Qiagen) for differentially expressed genes between cluster 1 and 2, 2 and 3 or 3 and 4 with *P* value calculated by Wilcoxon rank sum test and fold change of mean expression. Transcription factor binding motif analysis was conducted using HOMER software version 4.11(Heinz et al., 2010). Motifs were searched against DNA sequences from -300 to +50 around the transcription start sites of the differentially expressed genes between β-cell clusters. Upstream analysis for genes devided into 7 groups in pseudo-time heatmap was conducted using iReguron (Janky et al., 2014). The candidate upstream transcription factors which were also included in the group of the same expression pattern (i.e., decreased genes, groups 1-3; transiently up-regulated genes, group 4, 5; elevated genes, group 6-7) were listed.

Comparison of cluster4 genes with human datasets were performed using previously published dataset (Ackeifi et al., 2020; Arda et al., 2016; Wang et al., 2017). As for insulinoma dataset by Wang and juvenile human islet dataset by Arda, differentially expressed genes described in their reports were used. Genes upregulated in human islets treated by harmine were calculated by more than 2-fold elevation from expression values in the paper.

QUANTIFICATION AND STATISTICAL ANALYSIS.

Data of mouse phenotypes, immunohistochemical examinations and the proportion of each cluster in cell number of scRNA-seq (Figures 1C, 2C, S1A-S1D and S3C) are expressed as mean ± standard error of the mean (SEM). Comparison between two groups was performed by the Mann-Whitney U-test. The statistical analysis was carried out using GraphPad Prism software Version 8.0.2 (San Diego, CA, USA).

DATA AVAILABILITY

The accession number of NCBI Gene Expression Omnibus for scRNA-seq and bulk RNA-seq data reported in this manuscript is GSE152730 and GSE152731, respectively.

SUPPREMENTAL REFERENCES

Ackeifi, C., Swartz, E., Kumar, K., Liu, H., Chalada, S., Karakose, E., Scott, D.K., Garcia-Ocana, A., Sanchez, R., DeVita, R.J., et al. (2020). Pharmacologic and genetic approaches define human pancreatic beta cell mitogenic targets of DYRK1A inhibitors. JCI Insight *5*.

Anders, S., Pyl, P.T., and Huber, W. (2015). HTSeq--a Python framework to work with high-throughput sequencing data. Bioinformatics *31*, 166-169.

Arda, H.E., Li, L., Tsai, J., Torre, E.A., Rosli, Y., Peiris, H., Spitale, R.C., Dai, C., Gu, X., Qu, K., et al. (2016). Age-Dependent Pancreatic Gene Regulation Reveals Mechanisms Governing Human beta Cell Function. Cell Metab *23*, 909-920.

Butler, A., Hoffman, P., Smibert, P., Papalexi, E., and Satija, R. (2018). Integrating single-cell transcriptomic data across different conditions, technologies, and species. Nat Biotechnol *36*, 411-420.

Heinz, S., Benner, C., Spann, N., Bertolino, E., Lin, Y.C., Laslo, P., Cheng, J.X., Murre, C., Singh, H., and Glass, C.K. (2010). Simple combinations of lineage-determining transcription factors prime cis-regulatory elements required for macrophage and B cell identities. Mol Cell *38*, 576-589.

Janky, R., Verfaillie, A., Imrichova, H., Van de Sande, B., Standaert, L., Christiaens, V., Hulselmans, G., Herten, K., Naval Sanchez, M., Potier, D., et al. (2014). iRegulon: from a gene list to a gene regulatory network using large motif and track collections. PLoS Comput Biol *10*, e1003731.

Love, M.I., Huber, W., and Anders, S. (2014). Moderated estimation of fold change and dispersion for RNA-seq data with DESeq2. Genome Biol *15*, 550.

Nestorowa, S., Hamey, F.K., Pijuan Sala, B., Diamanti, E., Shepherd, M., Laurenti, E., Wilson, N.K., Kent, D.G., and Gottgens, B. (2016). A single-cell resolution map of mouse hematopoietic stem and progenitor cell differentiation. Blood *128*, e20-31.

Pertea, M., Kim, D., Pertea, G.M., Leek, J.T., and Salzberg, S.L. (2016). Transcript-level expression analysis of RNA-seq experiments with HISAT, StringTie and Ballgown. Nat Protoc *11*, 1650-1667.

Peshavaria, M., Larmie, B.L., Lausier, J., Satish, B., Habibovic, A., Roskens, V., Larock, K., Everill, B., Leahy, J.L., and Jetton, T.L. (2006). Regulation of pancreatic beta-cell regeneration in the normoglycemic 60% partial-pancreatectomy mouse. Diabetes *55*, 3289-3298.

Qiu, X., Mao, Q., Tang, Y., Wang, L., Chawla, R., Pliner, H.A., and Trapnell, C. (2017). Reversed graph embedding resolves complex single-cell trajectories. Nat Methods *14*, 979-982.

Romagnoli, D., Boccalini, G., Bonechi, M., Biagioni, C., Fassan, P., Bertorelli, R., Sanctis, V., Leo, A.D., Migliaccio, I., Malorni, L., et al. (2018). ddSeeker: a tool for processing Bio-Rad ddSEQ single cell RNA-seq data. BMC Genomics *19*, 960.

Stuart, T., Butler, A., Hoffman, P., Hafemeister, C., Papalexi, E., Mauck, W.M., 3rd, Hao, Y., Stoeckius, M., Smibert, P., and Satija, R. (2019). Comprehensive Integration of Single-Cell Data. Cell *177*, 1888-1902 e1821.

Sutton, R., Peters, M., McShane, P., Gray, D.W., and Morris, P.J. (1986). Isolation of rat pancreatic islets by ductal injection of collagenase. Transplantation *42*, 689-691.

Tran, K.A., Pietrzak, S.J., Zaidan, N.Z., Siahpirani, A.F., McCalla, S.G., Zhou, A.S., Iyer, G., Roy, S., and Sridharan, R. (2019). Defining Reprogramming Checkpoints from Single-Cell Analyses of Induced Pluripotency. Cell Rep *27*, 1726-1741 e1725.

Trapnell, C., Cacchiarelli, D., Grimsby, J., Pokharel, P., Li, S., Morse, M., Lennon, N.J., Livak, K.J., Mikkelsen, T.S., and Rinn, J.L. (2014). The dynamics and regulators of cell fate decisions are revealed by pseudotemporal ordering of single cells. Nat Biotechnol *32*, 381-386.

Usui, R., Yabe, D., Fauzi, M., Goto, H., Botagarova, A., Tokumoto, S., Tatsuoka, H., Tahara, Y., Kobayashi, S., Manabe, T., et al. (2019). GPR40 activation initiates store-operated Ca(2+) entry and potentiates insulin secretion via the IP3R1/STIM1/Orai1 pathway in pancreatic beta-cells. Sci Rep *9*, 15562.

Wang, H., Bender, A., Wang, P., Karakose, E., Inabnet, W.B., Libutti, S.K., Arnold, A., Lambertini, L., Stang, M., Chen, H., et al. (2017). Insights into beta cell regeneration for diabetes via integration of molecular landscapes in human insulinomas. Nat Commun *8*, 767.

Young, M.D., Wakefield, M.J., Smyth, G.K., and Oshlack, A. (2010). Gene ontology analysis for RNA-seq: accounting for selection bias. Genome Biol *11*, R14.